New Motion Control with Inertia Identification Function Using Disturbance Observer

Ichiro Awaya, Yoshiki Kato, Iwao Miyake and Masami Ito*
Mitsubishi Heavy Indusries Ltd
Iwatsuka, Nakamura, Nagoya 453, Japan
*Nagoya University
Furo, Chikusa, Nagoya 464, Japan

Abstract: This paper presents a new motion control system which has a simple inertia identification function using the disturbance observer. In the proposed system, the disturbance observer is used for the inertia identification as well as for the disturbance compensation. The inertia value is obtained by using the orthogonality relation among the torque components of the estimated disturbance torque. An inertia term of both the torque feedforward control and the disturbance observer is automatically re-adjusted by using the identification. The proposed motion control system consists of four parts; velocity feedback control, inertia torque feedforward control, disturbance observer and inertia identification part. The experimental results show that the precise control is achieved by the proposed motion control system.

1 Introduction

In the recent motion control system, the disturbance observer[1],[2], has been used. By applying the disturbance observer, the accurate control can be realized. The disturbance observer is easy to build in a motion controller because it has the simple structure. Furthermore,the robustness against the inertia variation can be obtained[3]. Therefore, theoretically it is possible to design the motion control system even if the inertia value is uncertain. In the actual application, the time constant of the observer should be small, however, it is difficult to realize such small time constant because of an existence of the backlash/noise. Consequently, the compensation lag makes it difficult to compensate the inertia variation torque. In such cases, the inertia torque feedforward control with the inertia identification is also required. Conventionally, the identification method requires the complex algorithm[4].

In this paper, we propose the new inertia identification method using the disturbance observer. The proposed identification method is simple because the inertia value is calculated only by the signals of the disturbance observer. In the proposed method, the convergence to the actual inertia value is assured. The experiments are performed by controlling the DC-brushless servomotor. Digital signal processor(TMS320C25) is used to execute the identification algorithm as well as the control algorithm. The results show that the precise control is possible by using the proposed algorithm.

2 Disturbance Observer

An identification model which is used in this paper is a motion system in Fig.1. The equation of motion is expressed as:

$$J\frac{d\omega}{dt}=u-D\omega+T_C, \tag{1}$$

where,
ω:angular velocity,
J :inertia constant,
u :driving torque,
D :viscous coefficient,
T_C:constant disturbance torque.

The disturbance torque τ_d includes various torque components except the driving torque u. Then, τ_d can be expressed as:

$$\tau_d=-D\omega+T_C. \tag{2}$$

The disturbance observer is used to estimate the unknown variable τ_d. τ_d can be regarded as a constant variable during the sampling period because the sampling frequency is much higher than the disturbance variation. Therefore,

$$\frac{d\tau_d}{dt}=0. \tag{3}$$

From eqs.(1),(2)and (3), the state equation is given by

$$\frac{dx}{dt}=Ax+Bu \tag{4}$$

$$y=Cx \tag{5}$$

where,

$$\left.\begin{aligned} &x=(\omega,\tau_d)^T\\ &A=\begin{pmatrix}0 & 1/J\\ 0 & 0\end{pmatrix}\\ &B=(1/J,0)^T\\ &C=(1,0)^T\end{aligned}\right| \tag{6}$$

Using the state equation above, the minimal order observer which estimates τ_d can be constructed as follows:

$$\frac{dz}{dt}=-\lambda z+\lambda J_n\omega+u \tag{7}$$

0-7803-0582-5 /92$3.00©1992 IEEE

$$\tau_e = -\lambda z + \lambda J_n \omega \qquad (8)$$

where,
J_n:nominal inertia,
z :internal variable,
τ_e:estimated disturbance torque,
$-\lambda$:observer pole ($\lambda>0$).
By applying the Laplace transformation to eqs.(7) and (8), and combining, then:

$$\tau_e(s) = J_n \lambda \frac{s}{s+\lambda}\omega(s) - \frac{\lambda}{s+\lambda}u(s). \qquad (9)$$

Here, we introduce variables $q_0(t), q_1(t)$ as shown in eqs.(10) and (11)

$$\frac{dq_0}{dt} = -\lambda q_0 + \lambda u, \quad q_0(0)=0 \qquad (10)$$

$$\frac{dq_1}{dt} = -\lambda q_1 + \lambda \omega, \quad q_1(0)=0. \qquad (11)$$

Then, the estimated disturbance torque $\tau_e(t)$ is given by:

$$\tau_e(t) = J_n \dot{q}_1 - q_0, \quad \tau_e(0)=0. \qquad (12)$$

As the result, the block diagram of the disturbance observer is shown in Fig.2.

3 New Inertia Identification

3.1 Components of estimated disturbance torque

The inertia variation δJ is caused by a load change or by an estimate error of an inertia value, and is expressed as eq.(13):

$$\delta J = J - J_n. \qquad (13)$$

From eqs.(1),(7),(8) and (13), the following differential equation of $\tau_e(t)$ is derived as:

$$\frac{d\tau_e}{dt} = -\lambda \tau_e - \lambda(\delta J \dot{\omega} + D\omega - T_c). \qquad (14)$$

By using the variables $q_1(t)$ and $q_2(t)$, the estimated disturbance torque $\tau_{e(t)}$ is represented as follows:

$$\tau_e(t) = -\delta J \dot{q}_1(t) - D q_1(t) + T_c q_2(t) \qquad (15)$$

where, $q_2(t)$ is the variable which satisfies the following condition,

$$\frac{dq_2}{dt} = -\lambda q_2 + \lambda, \quad q_2(0)=0. \qquad (16)$$

In eq.(15), $\delta J \dot{q}_1(t)$ is the inertia variation torque, $Dq_1(t)$, the viscous torque and $T_c q_2(t)$ is the constant disturbance torque.

3.2 Test signal for inertia identification

Test signal for the inertia identification is the periodic velocity command as shown below:

$$r(t) = r(t-T), \quad r(t) \neq 0. \qquad (17)$$

where,
T:period of velocity command

3.3 Orthogonality relation

In the motion system driven by the velocity servo controller, the angular velocity $\omega(t)$ is the periodic signal in the steady-state when the test signal is applied. Therefore, the angular velocity $\omega(t)$ can be expressed as:

$$\lim_{t\to\infty}[\omega(t) - \omega(t-T)] = 0. \qquad (18)$$

The signal $q_{1(t)}$ is also periodic signal in the steady-state because input $\omega(t)$ is a periodic signal. Therefore,

$$\lim_{t\to\infty}[q_1(t) - q_1(t-T)] = 0. \qquad (19)$$

From eq.(16), the signal $q_2(t)$ approaches to 1 when t is ∞,

$$\left.\begin{array}{l} \lim_{t\to\infty} q_2(t) = 1 \\ \lim_{t\to\infty} \dot{q}_2(t) = 0 \end{array}\right\} \qquad (20)$$

Here, the inner product of signals $\varphi_a(t)$ and $\varphi_b(t)$ is defined as:

$$(\varphi_a, \varphi_b) = \int_{(k-1)T}^{kT} \varphi_a(t)\varphi_b(t)\,dt. \qquad (21)$$

Consequently, the signals $q_1(t)$ and $\dot{q}_1(t)$ satisfies the orthogonal condition defined by above inner product. Because the integration of $q_1(t)\dot{q}_1(t)$ by parts is expressed as:

$$\int_{(k-1)T}^{kT} q_1(t)\dot{q}_1(t)\,dt = \frac{q_1(kT)^2 - q_1((k-1)T)^2}{2}. \qquad (22)$$

Using eq.(19), we obtain the following orthogonality as:

$$\lim_{k\to\infty}\int_{(k-1)T}^{kT} q_1(t)\dot{q}_1(t)\,dt = 0. \qquad (23)$$

The inner product of the signals $q_2(t), \dot{q}_1(t)$ is expressed in the same way as:

$$\int_{(k-1)T}^{kT} q_2(t)\dot{q}_1(t)\,dt = [q_2(t)q_1(t)]_{(k-1)T}^{kT} - \int_{(k-1)T}^{kT} \dot{q}_2(t)q_1(t)\,dt. \qquad (24)$$

From eqs.(20) and (24), the orthogonality is:

$$\lim_{k\to\infty}\int_{(k-1)T}^{kT} q_2(t)\dot{q}_1(t)\,dt = 0. \qquad (25)$$

From eqs.(23)and(25), the signals $q_1(t)$ and $\dot{q}_1(t)$ as well as $q_2(t)$ and $\dot{q}_1(t)$ are orthogonal in the space defined by the inner product shown in eq.(21) in case of $k \to \infty$.

3.4 Inertia identification algorithm

The proposed algorithm consists of the following two steps.
(1st step)
Estimating the inertia variation δJ.
(2nd step)
Adding the estimated inertia variation δJ_e to the nominal inertia J_n.
To estimate the inertia value, the orthogonality relation derived above is used.

Two steps are represented in eqs.(26)and(27).

$$\delta J_e(k)=-\frac{\int_{(k-1)T}^{kT}\tau_e(t)\,\dot{q}_1(t)\,dt}{\int_{(k-1)T}^{kT}\dot{q}_1(t)^2dt},\ (k=1,2,\cdots) \tag{26}$$

$$J_e(k)=J_n+\delta J_e(k) \tag{27}$$

where,

$\delta J_e(k)$:estimated inertia variation at time kT,

$J_e(k)$:estimated inertia constant at time kT.

The block diagram representation of this identification is shown in Fig.3. The convergence of the estimated inertia value to the actual one is discussed next subsection.

3.5 Proof of convergence

The convergence of the estimated inertia value to the actual one is proved by using the orthogonality of eqs.(23) and (25). The proof is as follows:

Multiplying both sides of eq.(15) by $\dot{q}_1(t)$ and integrating by the time interval T give:

$$\begin{aligned}\int_{(k-1)T}^{kT}\tau_e(t)\,\dot{q}_1(t)\,dt=&-\delta J\int_{(k-1)T}^{kT}\dot{q}_1(t)^2\\ &-D\int_{(k-1)T}^{kT}q_1(t)\,\dot{q}_1(t)\,dt \\ &+T_C\int_{(k-1)T}^{kT}q_2(t)\,\dot{q}_1(t)\,dt.\end{aligned} \tag{28}$$

Substituting eqs.(23) and (25) into eq.(28) in case of $k\to\infty$, yields:

$$\begin{aligned}&\lim_{k\to\infty}\int_{(k-1)T}^{kT}\tau_e(t)\,\dot{q}_1(t)\,dt\\ &=-\delta J\lim_{k\to\infty}\int_{(k-1)T}^{kT}\dot{q}_1(t)^2dt.\end{aligned} \tag{29}$$

Consequently, δJ is obtained as follows:

$$\delta J=-\lim_{k\to\infty}\frac{\int_{(k-1)T}^{kT}\tau_e(t)\,\dot{q}_1(t)\,dt}{\int_{(k-1)T}^{kT}\dot{q}_1(t)^2dt} \tag{30}$$

From eqs.(26) and (30):

$$\lim_{k\to\infty}\delta J_e(k)=\delta J, \tag{31}$$

then,

$$\lim_{k\to\infty}J_e(k)=J. \tag{32}$$

Eq.(32) shows that the estimated inertia value $J_e(k)$ converges to the actual value. The identification time is adjustable because it depends on the period T.

4 Motion Control System

Fig.4 shows the motion control system. This system has four parts, (1)velocity feedback control, (2)inertia torque feedforward control, (3)disturbance observer and (4)inertia identification part. The identified inertia value is used for renewing the inertia term of both the torque feedforward control and the disturbance observer.

5 Experiment

5.1 Experimental system

Fig.5 shows the experimental system. The DC-brushless servomotor(360W) with a tachometer is driven by a servo amplifier. The load inertia is coupled to the servomotor through the reduction gear(gear ratio N is 2). The constant disturbance torque is simulated as Coulomb friction torque on the system, and it is generated by the brake mechanism. The angular velocity ω is detected by the tachometer and is sent to the 12bit-A/Dconverter. DSP(TMS320C25) is used to perform the functions as mentioned in this paper, they are, velocity control, disturbance torque compensation, inertia torque feedforward control and the inertia identification. The torque command is output from DSP through the 12bit-D/Aconverter.

5.2 Experimental results

The test signal for the inertia identification experiment is shown as:

$$r(t)=40+20\sin(2\pi t). \tag{33}$$

Parameters of the experimental system are shown as follows:

$$\left[\begin{array}{l}J_n=0\,(kg{\cdot}m^2)\quad (initial)\\ J=7.26\times10^{-3}\,(kg{\cdot}m^2)\\ \lambda=31.4\,(rad/s)\\ K_V=1\,(Nm{\cdot}s/rad)\end{array}\right.$$

Fig.6 shows the result without the friction. In the figure, the velocity feedback is performed in the period [a]. The inertia identification is performed in [b]. In this period, the relation between q_1 and $\dot{q}_1$ as well as q_2 and $\dot{q}_1$ are almost in the orthogonal condition. The torque feedforward control based on the identified inertia value is added in [c]. In [d], the inertia torque feedforward control as well as the disturbance compensation is also added.

The lines on the figure indicate the velocity error, the estimated disturbance torque τ_e, the test signal r and the response ω respectively. In the period [b], the maximum velocity error is 3.8(rad/s) and the estimated disturbance torque is existed, which is mainly caused by the inertia variation torque $\delta J\dot{\omega}$. After identification in the period [c], the velocity error is markedly reduced less than 1.7(rad/s) and the inertia variation torque $\delta J\dot{\omega}$ is no longer existed. This shows that the exact inertia identification is performed in this period by using the proposed algorithm. Furthermore, in [d], the velocity error is suppressed less than 0.7(rad/s) by the disturbance compensation.

Fig.7 shows the result with the friction. Similarly to the above result, the inertia variation torque $\delta J\dot{\omega}$ is not existed after the identification. The difference of the result is the existence of the constant torque component in the estimated disturbance torque. This component is caused by Coulomb friction torque (partly by viscous torque). This result shows that the inertia value can be estimated under

Coulomb friction torque. From Fig.7, Coulomb friction torque on the servomechanism is about 2.92(Nm).

6 Conclusion

In this paper, the motion control system based on new inertia identification by using a disturbance observer is proposed. The inertia identification method uses the signals of the disturbance observer. The convergence property is proved by using the orthogonality. The experimental results show that the inertia identification is correctly performed. The proposed control system can be implemented in a DSP controller. The simple and precise motion control system has realized.

References

[1] S.Komada and K.Ohnishi, "Force Feedback Control of Robot Manipulator by the Acceleration Tracing Orientation Method," IEEE Trans. on Industrial Electronics, vol.37,no.1, pp.6-12, 1990.

[2] J.Geerts and J.Scannell, "Application of Second Order Observers to Electro-Mechanical Servo Systems," JournalA, vol.31, no.3, pp85-90, 1990.

[3] M.Iwasaki and N.Matsui, "Robust Speed Control of IM with Torque Feedforward Control," Proc. of IEEE Int. Conf. on Industrial Electronics, Control and Instrumentation, 1991, pp.627-632.

[4] L.A.Dessaint, B.J.Hebert, H.Le-Huy and G.Cavuoti, "A DSP-Based Adaptive Controller for a Smooth Positioning System," IEEE Trans. on Industrial Electronics, vol.37, no.5, pp.372-377, 1990.

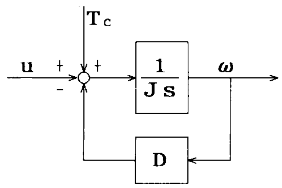

Figure 1:Identification model

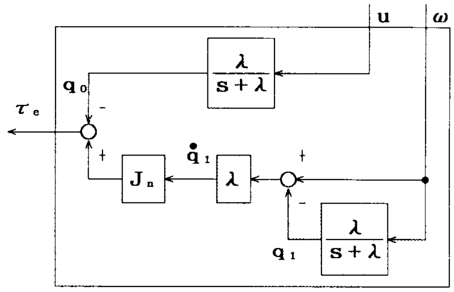

Figure 2:Disturbance observer

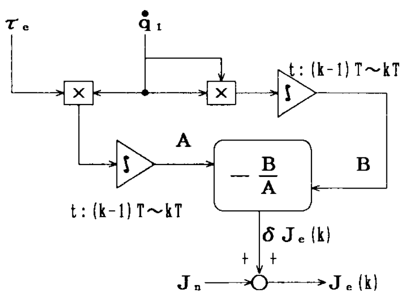

Figure 3:Block diagram of proposed identification method

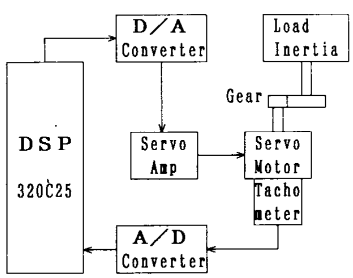

Figure 4:Experimental system

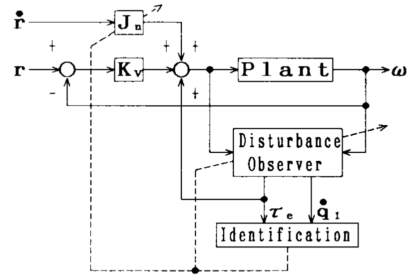

Figure 5:Motion control system with inertia identification

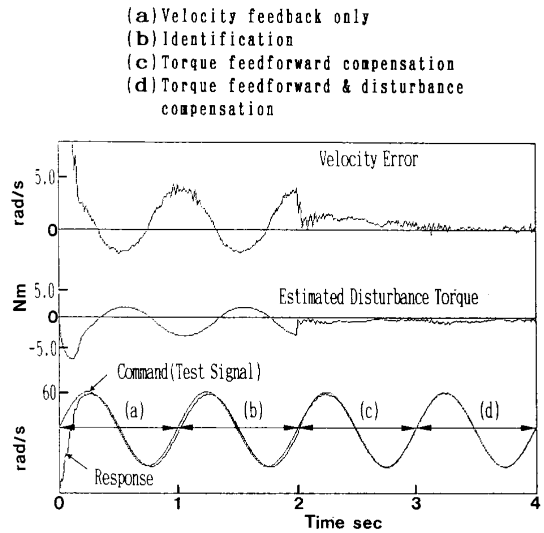

Figure 6:Experimental result without friction

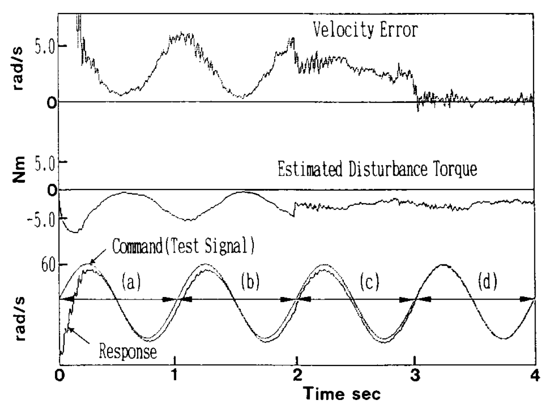

Figure 7:Experimental result with friction